Williams et al., http://www.jcb.org/cgi/content/full/jcb.201012116/DC1

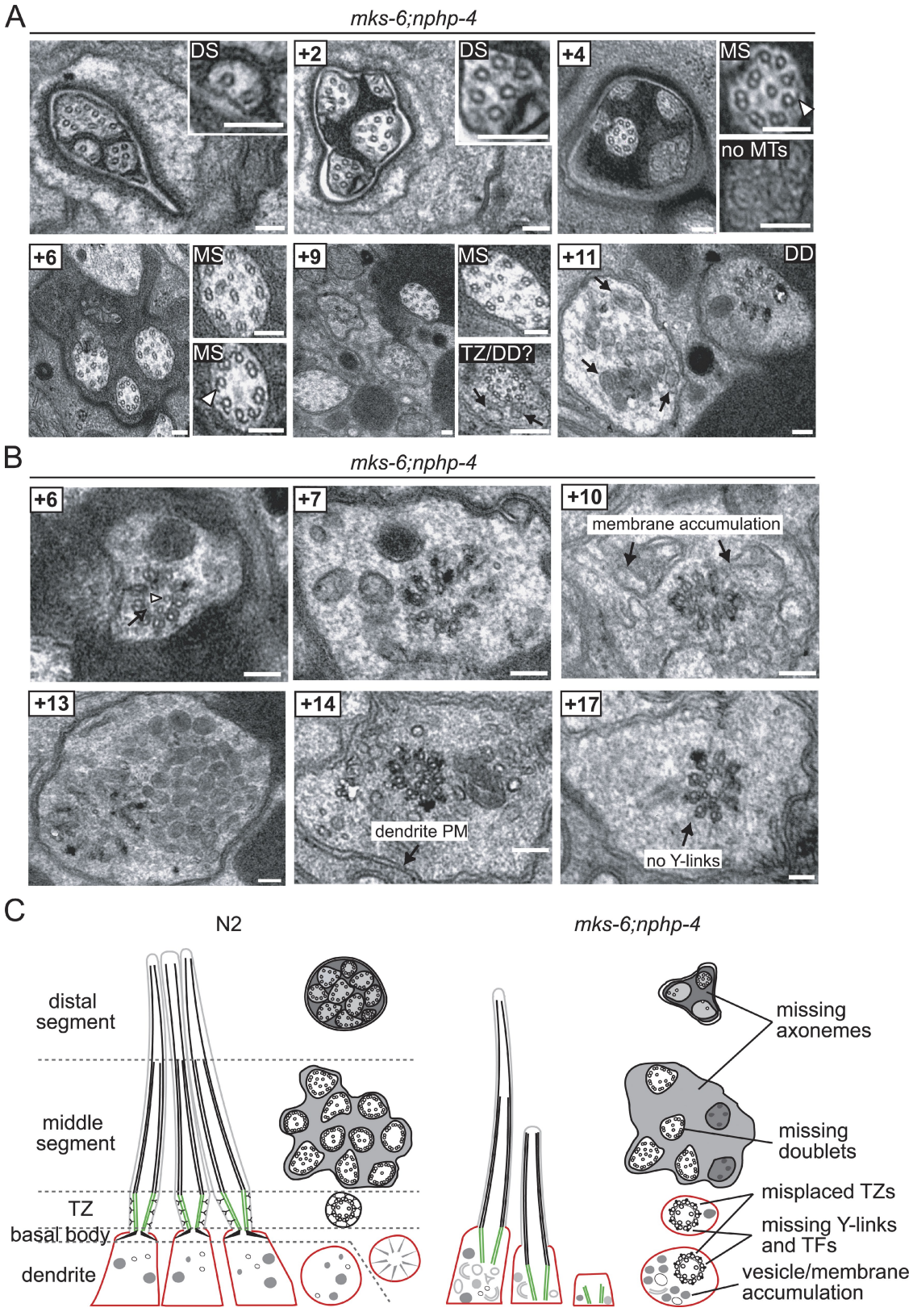

Figure S1. **Ultrastructural analysis of *mks-6;nphp-4* amphid channel cilia.** (A) Low and high magnification images of amphid channel cilia from TEM serial cross sections showing ciliary distal segments (DS), middle segments (MS), transition zones (TZ), and distal dendrite region (DD). Boxed number denotes proximal positioning of section relative to the top left section. Phenotypes observed include a reduced number of axonemes in distal region of amphid pore (3–4, instead of 10; +2, +4), axonemes lacking microtubules (MTs) altogether (+4; bottom inset) or possessing reduced MT doublet number (+6, bottom inset), unzipped microtubules (+4, +6; arrowheads), and no properly formed TZs at the distal tip of dendrites. Instead the TZs are misplaced in more proximal regions of the DD region (+9, +11) and no membrane-connecting Y-links are observed. In addition, the DD regions frequently contain abnormal accumulations of membranous-type material, some of which is highly electron dense and/or vesicular in nature (+9, +11; arrows). Bars, 100 nm. (B) High magnification images of misplaced TZs. These misplaced structures exhibit most of the features that define *C. elegans* TZs such as an apical ring membrane (+6; open arrow), which draws together outer doublet MTs with inner singlet MTs (+6; arrowhead) to form the characteristic constricted MT arrangement; however, Y-links and TFs are never observed (indicated in +17). In some cases, the TZ ring is incomplete, lacking 1–2 MT doublets (+7, and +11 in part A above). In most cases, large amounts of membranous-type material such as vesicles surround the misplaced TZs (indicated in +10). Dendritic plasma membrane (PM) indicated in +14. Bars, 100 nm. (C) Schematics of amphid channel cilia (longitudinal and transverse views) from N2 and *mks-6;nphp-4* worms showing the major ultrastructural defects observed (not to scale; e.g., TZs mispositioned even deeper than indicated).

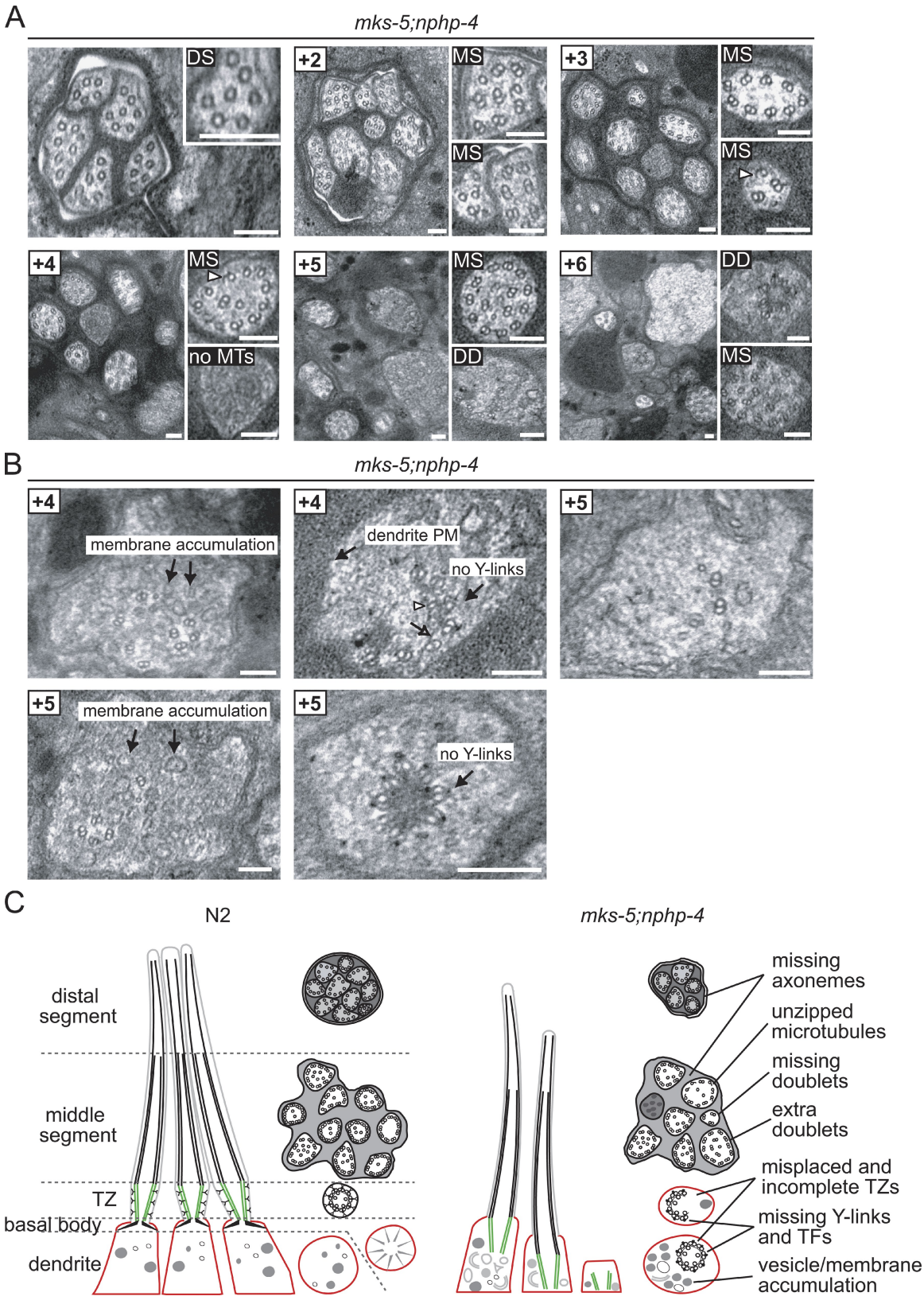

Figure S2. **Ultrastructural analysis of *mks-5;nphp-4* amphid channel cilia.** (A) Low and high magnification images of amphid channel cilia from TEM serial cross sections showing ciliary distal segments (DS), middle segments (MS), transition zones (TZ), and distal dendrite region (DD). Boxed number denotes proximal positioning of section relative to the top left section. Phenotypes observed include a reduced number of axonemes in distal region of amphid pore (5 instead of 10; top left panel), 1–2 axonemes missing in more proximal regions of pore (+3, +4), axonemes lacking microtubules (MTs; +4; bottom inset) or possessing abnormal MT doublet numbers (+3, both insets; +5, top inset; +6, bottom inset), or unzipped microtubules (arrowheads in +3, bottom inset; and +4, top inset). No properly formed TZs are observed at the distal tip of dendrites. Instead TZs are misplaced in more proximal regions of the DD region

(+5, bottom inset; +6 top inset) and there is evidence of incomplete formation of the MT ring (+5, bottom inset). In addition, DD regions sometimes contain abnormal accumulations of membranous-type material, some of which is highly electron dense and/or vesicular in nature (+5, bottom inset; +6, top inset). Bars, 100 nm. (B) High magnification images of misplaced TZs. These misplaced structures exhibit most of the features that define *C. elegans* TZs such as an apical ring membrane (indicated in +4; top middle image; open arrow), which draws together outer doublet MTs with inner singlet MTs (indicated in +4; top middle image; arrowhead) to form the characteristic constricted MT arrangement; however, Y-links and TFs are never observed (indicated in +4, top middle and +5, bottom right). In some cases, the TZ ring is incomplete, lacking MT doublets (+4, top middle). In other cases, MT doublets are not organized into symmetrical rings, indicating that these structures may not be TZs (+4, left; +5 top right image; +5, bottom left image). In many cases, large amounts of membranous-type material such as vesicles surround the misplaced TZs (indicated in +4, top left image and +5, bottom left image). Dendritic plasma membrane (PM) indicated in +4 (top middle image). Bars, 100 nm. (C) Schematics of amphid channel cilia (longitudinal and transverse views) from N2 and *mks-5;nphp-4* worms showing the major ultrastructural defects observed (not to scale; e.g., TZs mispositioned even deeper than indicated).

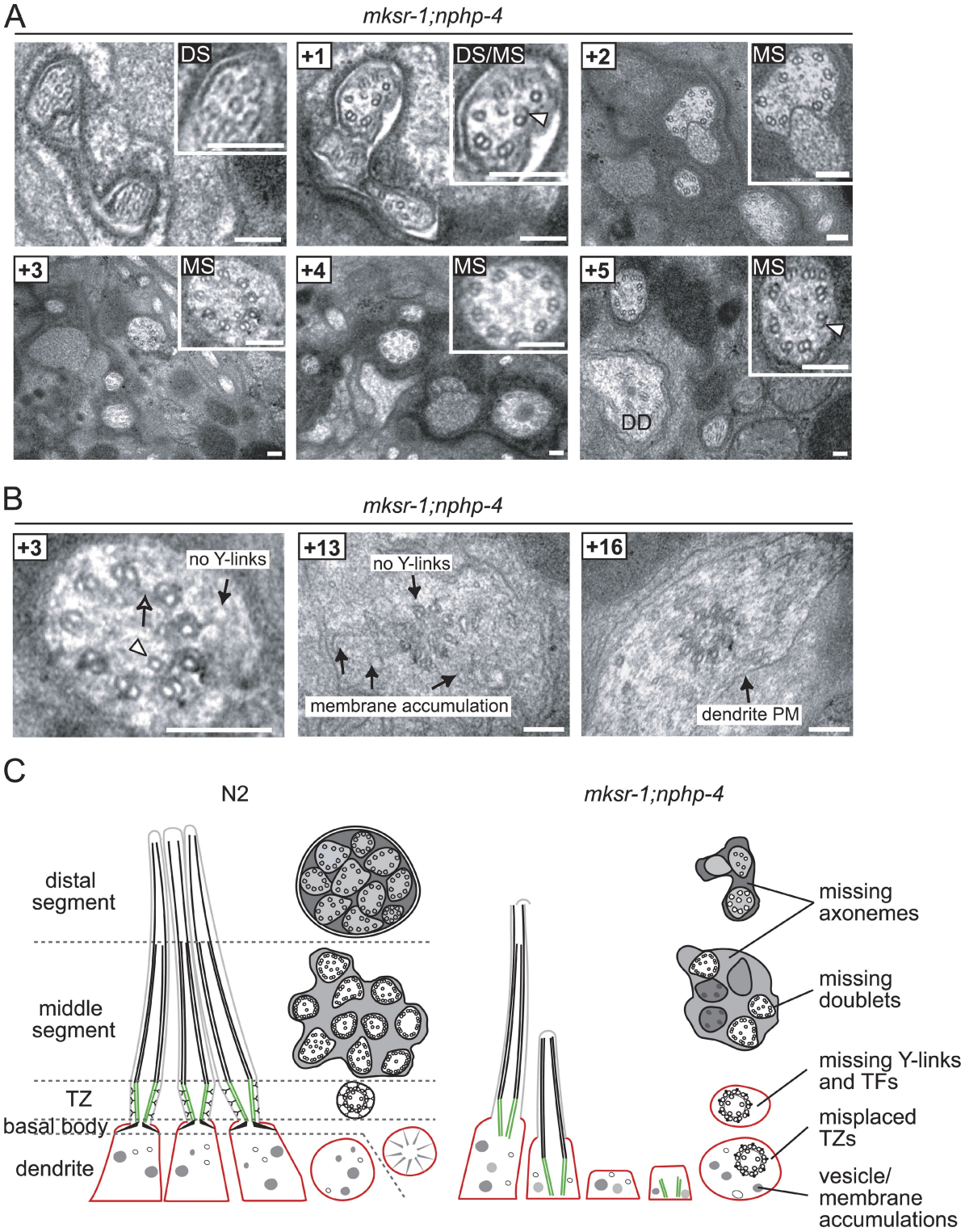

Figure S3. **Ultrastructural analysis of *mksr-1;nphp-4* amphid channel cilia.** (A) Low and high magnification images of amphid channel cilia from TEM serial cross sections showing ciliary distal segments (DS), middle segments (MS), transition zones (TZ), and distal dendrite region (DD). Boxed number denotes proximal positioning of section relative to the top left section. Phenotypes observed include a highly reduced number of axonemes in distal region (2–3, instead of 10; top left panel and +1) and proximal region of amphid pore (+2 to +4), axonemes lacking microtubules (MTs; +2), unzipped microtubules (+1; arrowheads), and TZs with no membrane connecting Y-links (+3, inset). Bars, 100 nm. (B) High magnification images showing TZ misplacement in more proximal regions of DD (+13, +16). Misplaced structures exhibit most of the features that define *C. elegans* TZs such as an apical ring membrane (+3; open arrow), which draws together outer doublet MTs with inner singlet MTs (+3; arrowhead) to form the characteristic constricted MT arrangement; however, Y-links and TFs are not observed (indicated in +3 and +13). Sometimes, abnormal accumulations of membranous-type material surround the misplaced TZs (indicated in +13). Dendritic plasma membrane (PM) indicated in +16. Bars, 100 nm. (C) Schematics of amphid channel cilia (longitudinal and transverse views) from N2 and *mksr-1;nphp-4* worms showing the major ultrastructural defects observed (not to scale; e.g., TZs mispositioned even deeper than indicated).

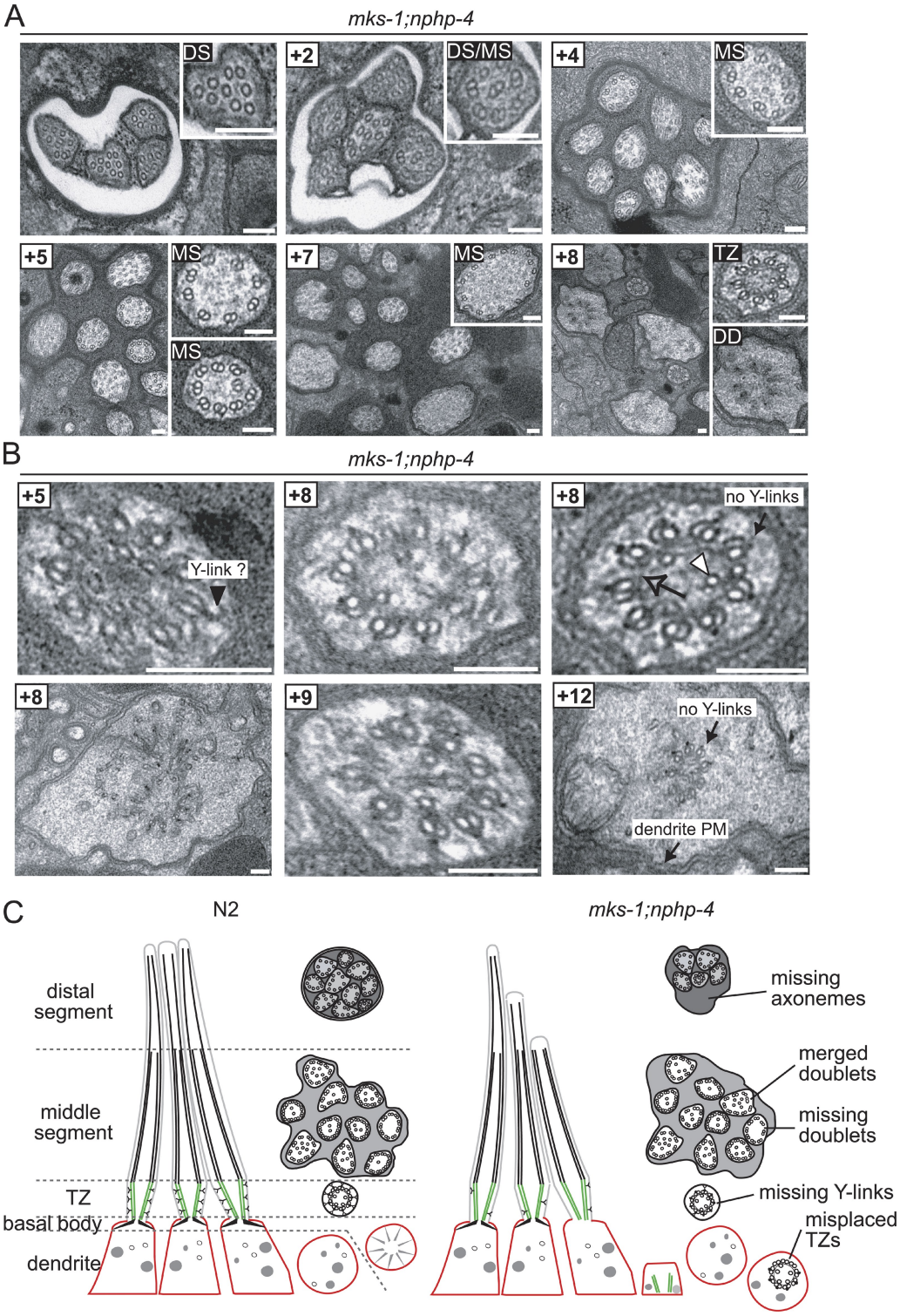

Figure S4. **Ultrastructural analysis of *mks-1;nphp-4* amphid channel cilia.** (A) Low and high magnification images of amphid channel cilia from TEM serial cross sections showing ciliary distal segments (DS), middle segments (MS), transition zones (TZ), and distal dendrite region (DD). Boxed number denotes proximal positioning of section relative to the top left section. Phenotypes observed include a moderate reduction in the number of axonemes in distal amphid pore (6, instead of 10; top left panel and +2), 1–2 axonemes missing in more proximal regions of pore (+4, +5), axonemes missing one or two outer MT doublets (+5; insets), and TZs that are sometimes misplaced in more proximal regions of DD (+8, bottom inset). Bars, 100 nm. (B) High magnification images of TZ structures. As indicated in +8 (top right image), and similar to wt worms, the TZ structures of *mks-6;nphp-4* animals consist of an apical ring membrane (open arrow) which draws together outer doublet MTs with inner singlet MTs (arrowhead) to form the characteristic constricted MT arrangement. However, although Y-links are sometimes observed (+5), they frequently are absent (indicated in +8; top right image and +12). Also, some TZs are misplaced in more proximal regions of DDs (+8; bottom left image and +12). Dendritic plasma membrane (PM) indicated in +12. (C) Schematics of amphid channel cilia (longitudinal and transverse views) from N2 and *mks-1;nphp-4* worms showing the major ultrastructural defects observed (not to scale; e.g., TZs mispositioned even deeper than indicated).

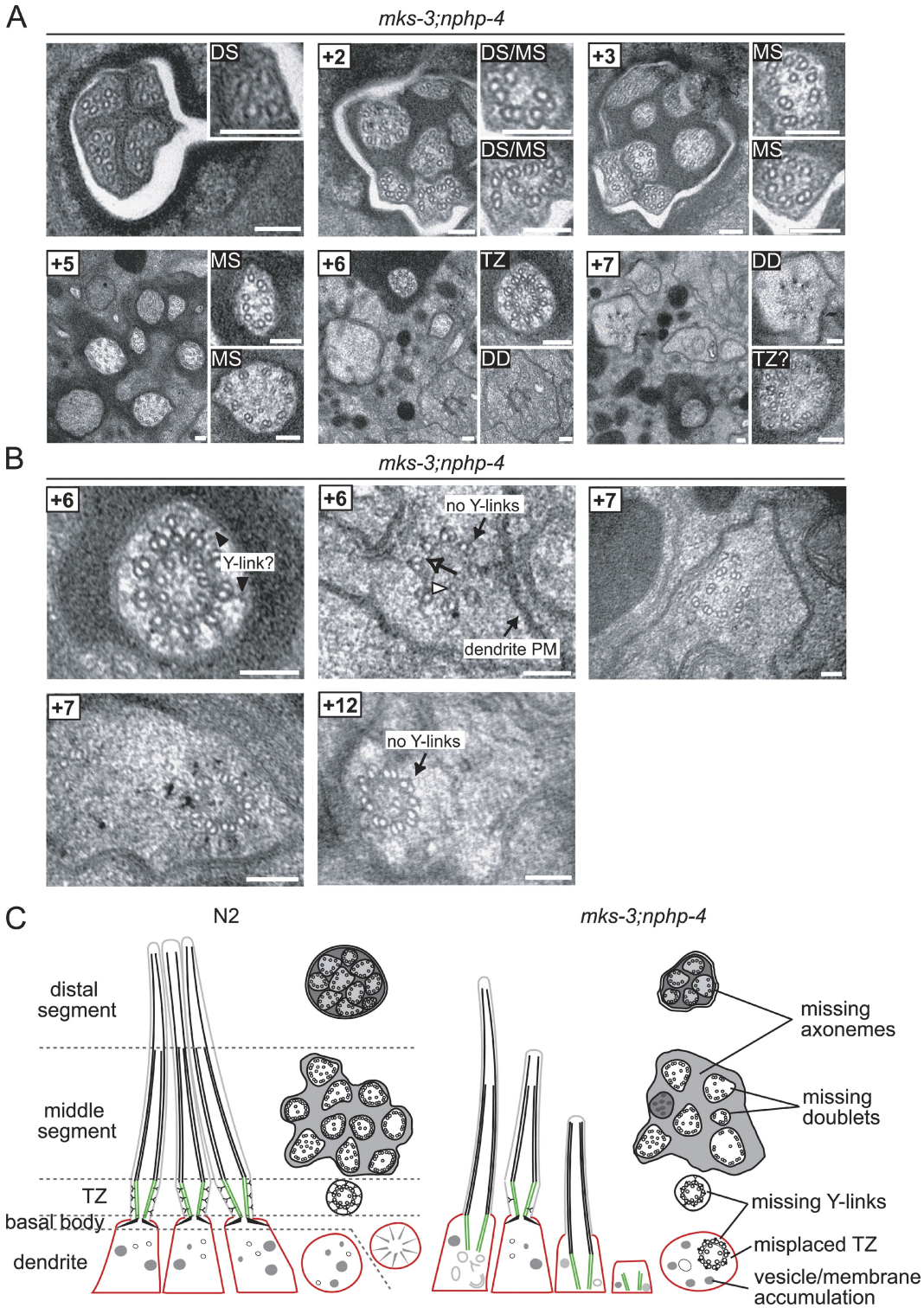

Figure S5. **Ultrastructural analysis of *mks-3;nphp-4* amphid channel cilia.** (A) Low and high magnification images of amphid channel cilia from TEM serial cross sections showing ciliary distal segments (DS), middle segments (MS), transition zones (TZ), and distal dendrite region (DD). Boxed number denotes proximal positioning of section relative to the top left section. Phenotypes observed include a moderate reduction in axoneme number in distal amphid pore (5, instead of 10; top left panel and +2), 2–3 axonemes missing in more proximal regions of pore (+3, +5), axonemes missing outer MT doublets (+3, +5; insets), and TZs misplaced in more proximal regions of DD (+7, top inset). Bars, 100 nm. (B) High magnification images showing that most TZs are misplaced in more proximal regions of DD. Misplaced structures exhibit characteristic features of *C. elegans* TZs such as an apical ring membrane (indicated in +6; top middle image; open arrow), which draws together outer doublet MTs with inner singlet MTs (indicated in +6; top middle image; arrowhead) to form the characteristic constricted MT arrangement; however, Y-links and TFs are typically never observed (indicated in +6; top middle image; and +12). In rarer cases where the TZ is positioned at distal dendrite tip (+6; top left image), intact Y-links are not clearly evident, although remnants may be present. Also, some TZs may be missing at least one doublet MT (+6; top middle image, +7; both images, +12). Dendritic plasma membrane (PM) indicated in +6 (top middle image). Bars, 100 nm. (C) Schematics of amphid channel cilia (longitudinal and transverse views) from N2 and *mks-3;nphp-4* worms showing the major ultrastructural defects observed (not to scale; e.g., TZs mispositioned even deeper than indicated).

Table S1 is provided as an Excel file and shows (A) conserved transition zone proteins and reported physical interactions, (B) *C. elegans* strains used in this study, (C) genome-wide HMM search for *C. elegans* proteins containing B9- and C2-related domains, (D) intraflagellar transport rate analyses for wild-type and TZ protein-disrupted strains, and (E) lifespan measurements.